Inverse Bremsstrahlung Absorption

D. Turnbull,[1,*] J. Katz,[1] M. Sherlock,[2] L. Divol,[2] N. R. Shaffer,[1] D. J. Strozzi,[2] A. Colaïtis,[3] D. H. Edgell,[1] R. K. Follett,[1] K. R. McMillen,[1] P. Michel,[2] A. L. Milder,[4] and D. H. Froula[1]

[1]*University of Rochester Laboratory for Laser Energetics, Rochester 14623, New York, USA*
[2]*Lawrence Livermore National Laboratory, Livermore 94550, California, USA*
[3]*Centre Lasers Intenses et Applications, Talence 33400, France*
[4]*University of Alberta, Edmonton, Alberta T6G 2R3, Canada*

(Received 10 January 2023; accepted 20 March 2023; published 4 April 2023)

Inverse bremsstrahlung absorption was measured based on transmission through a finite-length plasma that was thoroughly characterized using spatially resolved Thomson scattering. Expected absorption was then calculated using the diagnosed plasma conditions while varying the absorption model components. To match data, it is necessary to account for (i) the Langdon effect; (ii) laser-frequency (rather than plasma-frequency) dependence in the Coulomb logarithm, as is typical of bremsstrahlung theories but not transport theories; and (iii) a correction due to ion screening. Radiation-hydrodynamic simulations of inertial confinement fusion implosions have to date used a Coulomb logarithm from the transport literature and no screening correction. We anticipate that updating the model for collisional absorption will substantially revise our understanding of laser-target coupling for such implosions.

DOI: 10.1103/PhysRevLett.130.145103

In long-pulse laser-plasma experiments, inverse bremsstrahlung (IB) absorption is typically the dominant mechanism coupling laser energy to the plasma, and is often the only mechanism taken into account in models. This is true for the conventional approaches to every branch of inertial confinement fusion. Despite its importance, there remains no consensus on how to calculate IB absorption. In particular, absorption rates are proportional to the Coulomb logarithm, also known as the Gaunt factor, which has myriad definitions [1–9]. Moreover, calculations often include a Langdon absorption-reduction factor which assumes that laser-heated electron distribution functions (EDFs) become super-Gaussian [10]. Although recent measurements have confirmed the existence of such EDFs [11,12], attempts to validate the absorption-reduction factor itself have been fewer.

In this Letter, we present measurements of IB absorption and compare to predictions using various models. The precision of both the absorption measurements and the spatially resolved plasma conditions that serve as inputs to the model predictions enables us to discriminate between theories. We find that accounting for the Langdon effect is essential, even for moderate intensities and low-Z ions. We also find that the maximum impact parameter in the Coulomb logarithm for IB absorption should depend on the laser frequency rather than the plasma frequency, which is consistent with most bremsstrahlung-specific models [1–5,7] but different from Coulomb logarithms used for transport processes such as electron-ion temperature relaxation or heat conductivity [6,8]. Finally, even for the very underdense plasmas studied here ($n_e/n_c < 0.04$, where n_e is the electron density normalized by the critical density n_c), it is necessary to include a correction for ion screening, and we propose a suitable form.

The measurements were obtained on the OMEGA laser system at the University of Rochester's Laboratory for Laser Energetics using the laser-plasma instability platform. While the setup for the absorption campaigns was described more fully in Ref. [13], we briefly summarize the essential ingredients here. A supersonic gas jet with a 1-mm-outlet-diam nozzle emitted a narrow column of gas at target chamber center. The gas was ionized and preheated by thirteen 351-nm beams at $t = 0$ ns, each of which had a 500-ps-square pulse shape. The energy in each beam was a primary variable and ranged from 35 to 190 J per beam. A 527-nm probe beam with energy ranging from 1 to 4 J in a 100-ps Gaussian picket pulse was then injected from the P9 port into the plasma. Thomson-scattered light from that probe beam was collected using the imaging Thomson scattering system [14], which spatially resolved the plasma conditions over a distance of about 1.5 mm. Other campaign variables included probe timing (0.3 ns—during the heater beams, or 0.6 ns—after the heater beams, where the timing refers to the point at which the laser power reaches 2% of the peak power); gas composition (H_2, CH_4, or a mixture of 45% N_2 and 55% H_2); and gas jet backing pressure to vary the peak plasma density ($0.0037 < n_e/n_c < 0.036$).

The transmission, T, of the probe beam was determined by comparing an upstream measurement (off an uncoated wedged pickoff located in the P9 beam just before the target chamber) to a downstream measurement after target chamber center using the P9 transmitted beam diagnostic

(TBD) [15]. The ratio of these detectors was calibrated each day using a pair of shots through vacuum with an otherwise identical setup, so that data shots differed only by the presence of the absorbing plasma. Special care was taken to remain below threshold for potentially confounding sources of loss such as backscatter (monitored and maintained below a noise floor of ≈0.1%) and beam spray [16], as well as possible absorption-enhancement mechanisms like the return-current instability [17]. This was achieved by minimizing the probe intensity (while maintaining good Thomson-scattering signals) and peak plasma density (while still getting measurable absorption), and by selecting gases with a high hydrogen fraction to ensure strong ion-acoustic-wave damping. With competing losses kept small, the absorption A was simply $1-T$, with an estimated uncertainty of $(+0.07\%, -0.12\%)$ [13].

Other details of the setup varied slightly between three configurations. In config. No. 1 [Fig. 1(a)], all beams were pointed 1 mm above the exit face of the gas jet nozzle. The preheating beams were conditioned with full smoothing by spectral dispersion (SSD) and elliptical E-IDI-300 distributed phase plates (DPPs) oriented to complement the SSD such that each beam's profile was approximately round with a FWHM diameter just over 200 μm. The probe beam was conditioned with a CircSG100 DPP to have a 97-μm-FWHM diameter, and the Thomson scattering system field-of-view (TSS FOV) was centered around target chamber center. In config. No. 2, SG5-850 DPPs (714-μm-FWHM) conditioned the preheating beams without SSD to heat the entire plasma more uniformly, all beams were pointed 1.5 mm from the gas jet to improve beam clearance and reduce noise on the ion-feature Thomson scattering, and the TSS FOV was biased 300 μm toward the probe entrance to better capture the low-density tail on one side of the plasma. Cylindrical axisymmetry of the gas or plasma density about the gas jet axis allowed us to mirror those measurements onto the probe exit side while introducing minimal error. The probe was conditioned with a CircSG200 DPP to have a 165-μm-FWHM diameter. Finally, config. No. 3 was identical to config. No. 2 except for the use of a refractive (rather than reflective) Thomson-scattering collection telescope; its larger (> 4 mm) FOV eliminated the need for the axisymmetric assumption.

A sample characterized plasma profile is shown in Fig. 1(b). For the shots that included mid-Z ions, the ionization state was determined using FLYCHK [18]. Note that the plasmas were finite in length and measured almost in their entirety, so the absorption calculations are well constrained.

We can then use the measured plasma conditions to predict how much absorption should occur as the probe beam propagates through the plasma. Including corrections for both the Langdon effect (f_L) and ion screening (f_{sc}), the absorption rate (with units m^{-1}) is

$$\kappa = \nu_{ei} \frac{n_e/n_c}{c\sqrt{1-n_e/n_c}} f_L f_{sc}, \tag{1}$$

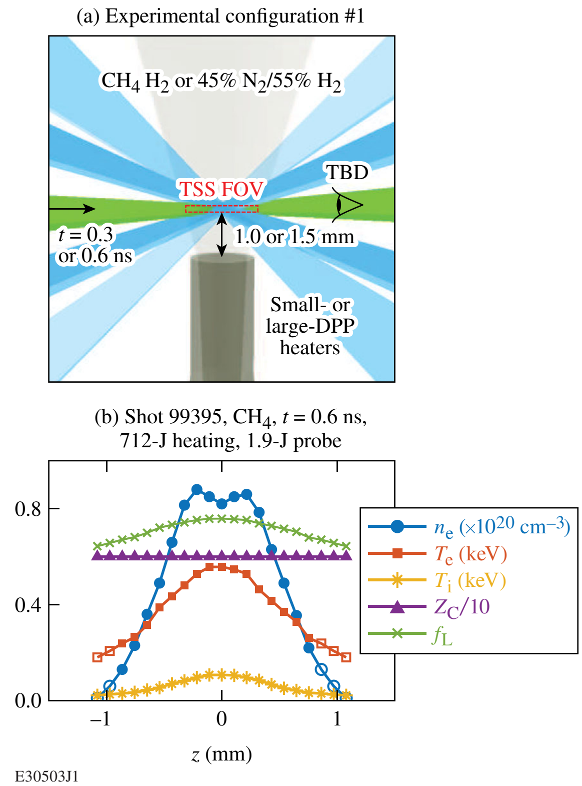

FIG. 1. An example experimental setup (config. No. 1) is shown in (a). An example of the measured plasma conditions is shown in (b). For density and temperature, solid markers denote points that were explicitly measured by Thomson scattering. Open markers indicate extrapolations based on the measured profile.

where $\nu_{ei} = 2.91\times10^{-12} T_e^{-3/2} \Sigma_i (Z_i^2 n_i \ln\Lambda_{IB,i})$ is the electron-ion collision rate including the summation over all ion species. (SI units are used throughout this Letter with the exception of temperatures in eV.)

The Coulomb logarithm generally arises from the need to bound an integral in the classical derivation for the electron-ion collision rate using maximum and minimum impact parameters $b_{\max}$ and $b_{\min}$, but one or both are ostensibly constrained depending on the derivation. While the following list is by no means exhaustive, it aims to include some of the better known theories while also spanning some key differences across all theories.

$$\text{Sommerfeld-Maue [1, 19]:}\quad \frac{\pi}{\sqrt{3}} \langle g_{ff} \rangle [f_e(v), \omega, Z], \tag{2}$$

$$\text{Oster [2]:}\quad \ln\left(\left(\frac{2}{e^{\gamma}}\right)^{5/2} \frac{v_t/\omega}{\max\left(\frac{Ze}{4\pi\epsilon_0 T_e}, \frac{\hbar}{1.68\sqrt{m_e T_e e}}\right)}\right), \tag{3}$$

$$\text{Lee-More [6]:}\quad \ln\left(\frac{\lambda_{D,ei}}{\max\left(\frac{Ze}{12\pi\epsilon_0 T_e}, \frac{\hbar}{2\sqrt{3 m_e T_e e}}\right)}\right), \tag{4}$$

$$\text{Dimonte-Daligault [8]: } \ln\left(1+0.7\frac{\lambda_{D,e}}{Ze/(4\pi\epsilon_0 T_e)}\right), \quad (5)$$

Sommerfeld's seminal result—a function of the EDF $f_e(v)$, laser frequency ω, and Z—is an exact quantum-mechanical solution for the bremsstrahlung emitted in a single binary electron-ion collision, but it is in terms of complicated hypergeometric functions that can be computationally prohibitive to evaluate [1]. However, there have been many approximations to Sommerfeld over the ensuing century [19–24]. To estimate Sommerfeld in our analysis, we use Pradler's Eq. (12) for the thermally averaged Gaunt factor, which in turn uses their Eq. (10) for the fitting formula to the velocity-dependent Gaunt factor [19]. Oster [Eq. (3)] was also derived from a binary-collision approach, but additional assumptions (straight-line approximation to the hyperbolic trajectory) facilitated a much simpler formula [2]. In the leading order-unity term, $\gamma = 0.577$ is Euler's constant. It is otherwise written in terms of a maximum impact parameter v_t/ω where $v_t = \sqrt{T_e e/m_e}$ is the electron thermal velocity, and a minimum impact parameter that is either classical (the distance of closest approach) or quantum-mechanical (related to the thermal de Broglie wavelength). In the quantum limit, it simplifies considerably to $\ln(4T_e e/\hbar\omega e^\gamma)$, which is found elsewhere in the literature [7,25,26]. Though not shown, the well-known formula for the high-frequency limit (when $\omega \gg \omega_p$, where ω_p is the plasma frequency) from Dawson-Oberman [3], later revised by Johnston [5] and adopted by the NRL plasma formulary [27], has the same format as Oster but lacks the order-unity terms to reflect the indeterminacy of $b_{\min}$ in that derivation, although $b_{\max}$ was rigorously derived. They could instead have chosen minimum impact parameters in order to match the results of Oster. The justification offered in the bremsstrahlung literature for this common $b_{\max}$ is that the collision time must be short compared to the period of the wave, otherwise the heating is rendered ineffective. (Note that —given the laser-frequency dependence—the Coulomb logarithm is expected to be specific to each beam in the case of overlapping beams with different frequencies.)

For transport processes such as electron thermal conductivity [6] or electron-ion temperature relaxation [8], however, it is typical to assume a Debye length for the maximum impact parameter, with Lee-More [Eq. (4)] allowing ions to participate in the shielding (giving $\lambda_{D,ei} = \sqrt{(\epsilon_0 T_e T_i / n_e e(ZT_e + T_i))}$) whereas Dimonte-Daligault [Eq. (5)] concluded that ions do not participate (therefore $\lambda_{D,e} = \sqrt{(\epsilon_0 T_e/n_e e)} = v_t/\omega_p$). Although transport Coulomb logarithms are not necessarily relevant to IB absorption, the community has not maintained a clear distinction between the two, and as we will discuss later, Lee-More has long been used to compute IB absorption in the codes that simulate inertial confinement fusion experiments. The various theories also differ by other numerical factors inside the logarithm.

The Langdon absorption-reduction factor is

$$f_L = 1 - 0.553/[1 + (0.27/\alpha)^{0.75}], \quad (6)$$

where $\alpha = Z_{\text{eff}} v_o^2/v_t^2$, $Z_{\text{eff}} = \langle Z^2\rangle/\langle Z\rangle$, and v_o is the oscillatory velocity of electrons in the laser field [10]. The factor assumes that EDFs become increasingly non-Maxwellian at high laser intensity. Matte *et al.* later showed using Fokker-Planck simulations that the bulk electrons relevant to IB absorption conform to a super-Gaussian EDF with an exponent given by $m(\alpha) = 2 + 3/(1 + 1.66/\alpha^{-0.724})$, and they stated that such EDFs are consistent with the Langdon factor to within 1% for any α [28]. While we have consistently verified the Matte formula when we have sensitivity to the EDF with Thomson scattering [11,12], the absorption-reduction factor itself has not yet been directly validated. All of the Thomson-scattering analysis here assumes super-Gaussian EDFs with α determined by the instantaneous overlapped intensity, i.e., the probe only (at $t = 0.6$ ns) or an effective intensity summing the probe and the preheating beams [multiplied by $(2/3)^2$ in order to be "2ω equivalent" since $v_o \propto \omega^{-1}$ in the Langdon factor] if co-timed.

Finally, although the Coulomb logarithms based on binary collisions (Sommerfeld, Oster) neglected medium effects, and we can conclude from Dawson's work that medium effects are not important in the high-frequency limit [3,29], it seems apparent from molecular dynamics (MD) simulations [9] and partial wave calculations of screened Coulomb potentials [30] that ion screening becomes important for densities of interest above $n_e \gtrsim 0.01 n_c$. To account for this, we define the screening correction factor

$$f_{sc} = \frac{ln\left(\frac{2T_e e}{\hbar\omega}\frac{y}{\sqrt{1+y^2}}\right) - \frac{1}{2(1+y^2)}}{ln(\frac{2T_e e}{\hbar\omega})}, \quad (7)$$

where $y = l_{sc}/b_{\max} = l_{sc}\omega/v_t$ is the ratio of the effective screening length to the maximum impact parameter. This term is Rozsnyai's (simplified) Gaunt factor [31] normalized by the Gaunt factor derived in the Born approximation without screening, and is valid for $y \geq 0.005$ and $\hbar\omega \ll T_e e$, which applies to most laser-produced plasmas. Although the Debye length is the most common choice for the screening length in weakly coupled plasmas, we choose instead the mean interionic distance, or Wigner-Seitz radius, $l_{sc} = a_i = (3/4\pi n_i)^{1/3}$ where n_i is the average ion density, in order to match the data. This factor reproduces the differences between screened and unscreened Coulomb potentials for the weakly coupled examples in Ref. [30] very well. A qualitative explanation for the impact of screening in the case when $a_i < b_{\max}$ is that electrons interact with more than one ion simultaneously when the ions are relatively closely

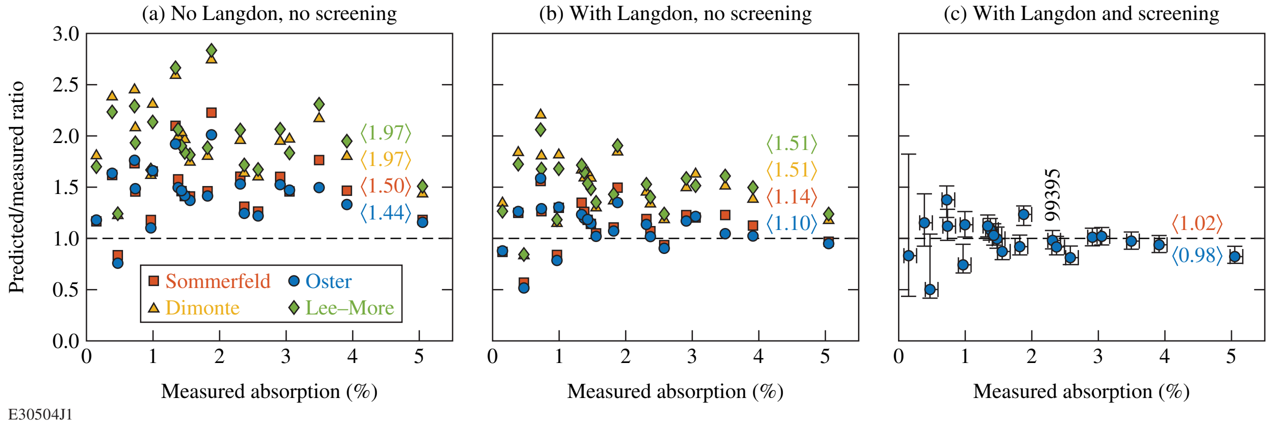

FIG. 2. Ratios of predicted-to-measured absorption for twenty-two distinct OMEGA shots (a) without the Langdon factor or screening correction; (b) with Langdon but no screening; or (c) accounting for both the Langdon effect and ion screening, along with the uncertainty. Only Oster is shown here so that the uncertainty can be seen more clearly, but the agreement is comparable for Sommerfeld.

spaced (see, e.g., Ref. [32], where the particles are stars in that case). While previous molecular dynamics simulations of absorption have covered the strongly coupled regime well [33], the choice of $f_{sc}(a_i)$ we offer as the best fit to the data should motivate further MD simulations and theoretical analysis in the more computationally demanding regime of weakly coupled plasmas to more accurately determine the effect of close ion spacing.

Predictions using various permutations of the above theories are compared to measurements in Fig. 2 along with the averages of the predicted-to-measured ratios for each model. Measured absorption ranged from 0.15% to 5% due to variation in Z, n_e, T_e, and laser intensity, with the best data in the range of $1\% < A < 4\%$ for a peak density around $n_e \approx 0.02 n_c$ where measured absorption was large compared to the experimental uncertainty but laser-plasma-instability risk remained small.

Figure 2(a) shows that all of the models overestimate the absorption when neglecting both the Langdon and ion-screening correction factors. The average path-integrated Langdon factor for all of the data was 0.76, so predictions that include it begin to approach the data as shown in Fig. 2(b). Although it is often assumed that the Langdon effect is only relevant in high-Z plasmas, f_L averaged 0.81 and dropped as low as 0.74 even for the eight pure-hydrogen shots due largely to the overlapped intensity of the heater beams, with six of the eight shots being co-timed. It should always be taken into account.

More specifically, only the bremsstrahlung models (Sommerfeld and Oster) approach the data, whereas the transport theories (Lee-More and Dimonte-Daligault) are still off by $> 50\%$—a significant error in a logarithmic quantity. The difference arises primarily in the maximum impact parameters, the ratio of which is large $[\lambda_{D,e}/(v_t/\omega) = \sqrt{n_c/n_e} \approx 7]$ for these underdense plasmas. The results strongly suggest that the laser-frequency dependence in the bremsstrahlung models is in fact correct for IB absorption.

The differences between Sommerfeld and Oster are slight. When the quantum-mechanical minimum impact parameter was invoked (most cases of hydrogen), the two models were almost identical. Differences arose when the classical minimum impact parameter was invoked (all of the carbon and nitrogen collisions), suggesting close collisions that violate Oster's straight-line approximation are more important in those cases. For direct-drive inertial confinement fusion coronal plasma conditions, the quantum $b_{\min}$ is more relevant so Oster should suffice as a good approximation to Sommerfeld.

The average value of f_{sc} was 0.89, so the ion-screening correction factor is the final ingredient that brings predictions into agreement with the measurements [Fig. 2(c)], with Oster being on average just 2% below the data, and Sommerfeld just 2% above. We therefore conclude that Sommerfeld, with corrections for the Langdon effect and ion-screening, is likely the best model for IB absorption, but Oster reasonably approximates Sommerfeld in most situations. Had we used $f_{sc}(\lambda_{D,ei})$ instead of $f_{sc}(a_i)$, screening would be a much smaller (%-level) correction—not enough to match the data.

The implications for direct-drive inertial confinement fusion are significant. Accurately predicting time-dependent laser-target coupling has been a long-standing challenge. Early on, simulations were tuned using a variable flux limiter in the heat transport model. Later, when the nonlocal model removed the flux-limiter knob, a crossed-beam energy transfer (CBET) package was added to better match the data [34]. When discrepancies persisted, multipliers were added to the CBET model due to a legacy belief that laser-plasma instabilities are not well understood and difficult to model quantitatively [35]. However, focused experiments have shown that CBET can be calculated reliably when the plasma conditions are well known [11,36,37].

While the Langdon factor is generally used, radiation hydrodynamics have long defaulted to using Lee-More

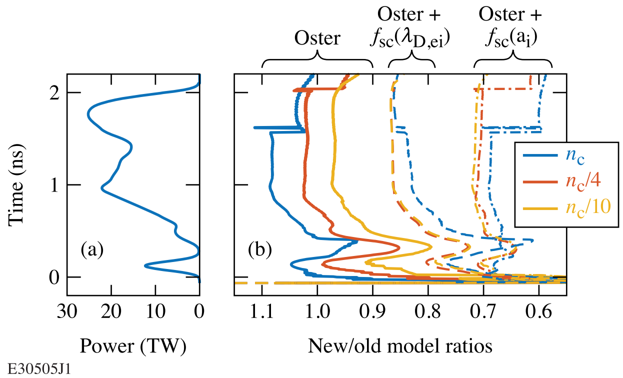

FIG. 3. (a) Pulse shape for shot 90288. (b) The expected impacts on the absorption rate for the proposed changes to the model as a function of time and space, where the old model included the Lee-More Coulomb logarithm and the Langdon factor.

without any ion-screening correction for IB absorption [38–40]. Figure 3 shows the impact of the proposed model changes using the well-known shot 90288 (described in Ref. [41]) as an example. Switching only from Lee-More to Oster would modestly redistribute absorption from lower density to higher density, which could actually benefit the implosion. However, the ion-screening correction systematically reduces absorption by about ≈15% to 20% when using the more conservative Debye length in the definition of y for Eq. (7), or ≈30% when using a_i as suggested by our data. These predictions entail considerable extrapolation from the relatively low densities of the gas-jet experiments up to the higher densities relevant for direct-drive implosions, but we expect that the same mechanisms (and no additional mechanisms) remain in play for IB absorption up to critical density. We therefore believe that a revised model motivated by the results presented here will substantially modify our understanding of direct-drive inertial confinement fusion.

This material is based upon work supported by the DOE NNSA under Grant No. DE-NA0003856, the University of Rochester, and the New York State Energy Research and Development Authority. This report was prepared as an account of work sponsored by an agency of the U.S. Government. Neither the U.S. Government nor any agency thereof, nor any of their employees, makes any warranty, express or implied, or assumes any legal liability or responsibility for the accuracy, completeness, or usefulness of any information, apparatus, product, or process disclosed, or represents that its use would not infringe privately owned rights. Reference herein to any specific commercial product, process, or service by trade name, trademark, manufacturer, or otherwise does not necessarily constitute or imply its endorsement, recommendation, or favoring by the U.S. Government or any agency thereof. The views and opinions of authors expressed herein do not necessarily state or reflect those of the U.S. Government or any agency thereof. This work was performed under the auspices of the U.S. Department of Energy by Lawrence Livermore National Laboratory under Contract No. DE-AC52-07NA27344.

*turnbull@lle.rochester.edu

[1] A. Sommerfeld and A. W. Maue, Ann. Phys. (Berlin) **414**, 629 (1935).
[2] L. Oster, Rev. Mod. Phys. **33**, 525 (1961).
[3] J. Dawson and C. Oberman, Phys. Fluids **5**, 517 (1962).
[4] R. E. Kidder, in Proceedings of the International School of Physics "Enrico Fermi", *Physics of High Energy Density* (Academic Press, New York, 1971).
[5] T. W. Johnston and J. M. Dawson, Phys. Fluids **16**, 722 (1973).
[6] Y. T. Lee and R. M. More, Phys. Fluids **27**, 1273 (1984).
[7] S. Skupsky, Phys. Rev. A **36**, 5701 (1987).
[8] G. Dimonte and J. Daligault, Phys. Rev. Lett. **101**, 135001 (2008).
[9] R. Devriendt and O. Poujade, Phys. Plasmas **29**, 073301 (2022).
[10] A. B. Langdon, Phys. Rev. Lett. **44**, 575 (1980).
[11] D. Turnbull, A. Colaitis, A. M. Hansen, A. L. Milder, J. P. Palastro, J. Katz, C. Dorrer, B. E. Kruschwitz, D. J. Strozzi, and D. H. Froula, Nat. Phys. **16**, 181+ (2020).
[12] A. L. Milder, J. Katz, R. Boni, J. P. Palastro, M. Sherlock, W. Rozmus, and D. H. Froula, Phys. Rev. Lett. **127**, 015001 (2021).
[13] J. Katz, D. Turnbull, S. T. Ivancic, A. L. Milder, and D. H. Froula, Rev. Sci. Instrum. **93**, 123510 (2022).
[14] J. Katz, R. Boni, C. Sorce, R. Follett, M. J. Shoup, and D. H. Froula, Rev. Sci. Instrum. **83**, 10E349 (2012).
[15] J. Katz, D. Turnbull, B. E. Kruschwitz, A. L. Rigatti, R. Rinefierd, and D. H. Froula, Rev. Sci. Instrum. **92**, 033526 (2021).
[16] D. Turnbull, J. Katz, D. E. Hinkel, P. Michel, T. Chapman, L. Divol, E. Kur, S. MacLaren, A. L. Milder, M. Rosen, A. Shvydky, G. B. Zimmerman, and D. H. Froula, Phys. Rev. Lett. **129**, 025001 (2022).
[17] A. L. Milder, J. Zielinski, J. Katz, W. Rozmus, D. Edgell, A. Hansen, M. Sherlock, C. Bruulsema, J. P. Palastro, D. Turnbull, and D. H. Froula, Phys. Rev. Lett. **129**, 115002 (2022).
[18] H.-K. Chung, M. Chen, W. Morgan, Y. Ralchenko, and R. Lee, High Energy Density Phys. **1**, 3 (2005).
[19] J. Pradler and L. Semmelrock, Astrophys. J. **922**, 57 (2021).
[20] W. J. Karzas and R. Latter, Astrophys. J. Suppl. Ser. **6**, 167 (1961), https://ui.adsabs.harvard.edu/abs/1961ApJS....6..167K/abstract.
[21] P. J. Brussaard and H. C. van de Hulst, Rev. Mod. Phys. **34**, 507 (1962).
[22] J. R. Stallcop and K. W. Billman, Plasma Phys. **16**, 1187 (1974).
[23] R. Marchand and C. Capjack, Comput. Phys. Commun. **38**, 357 (1985).

[24] P. A. M. van Hoof, R. J. R. Williams, K. Volk, M. Chatzikos, G. J. Ferland, M. Lykins, R. L. Porter, and Y. Wang, Mon. Not. R. Astron. Soc. **444**, 420 (2014).

[25] G. Bekefi, *Radiation Processes in Plasmas* (John Wiley and Sons, Inc., New York, 1966).

[26] R. Kidder, Nucl. Fusion **8**, 3 (1968).

[27] A. S. Richardson, *2019 NRL Plasma Formulary* (Naval Research Laboratory, Washington, DC, 2019).

[28] J. P. Matte, M. Lamoureux, C. Moller, R. Y. Yin, J. Delettrez, J. Virmont, and T. W. Johnston, Plasma Phys. Controlled Fusion **30**, 1665 (1988).

[29] J. Dawson and C. Oberman, Phys. Fluids **6**, 394 (1963).

[30] G. Armstrong, J. Colgan, D. Kilcrease, and N. Magee, High Energy Density Phys. **10**, 61 (2014).

[31] B. F. Rozsnyai, J. Quant. Spectrosc. Radiat. Transfer **22**, 337 (1979).

[32] S. Chandrasekhar, *Principles of Stellar Dynamics* (The University of Chicago Press, Chicago, 1942).

[33] S. Pfalzner and P. Gibbon, Phys. Rev. E **57**, 4698 (1998).

[34] I. V. Igumenshchev, D. H. Edgell, V. N. Goncharov, J. A. Delettrez, A. V. Maximov, J. F. Myatt, W. Seka, A. Shvydky, S. Skupsky, and C. Stoeckl, Phys. Plasmas **17**, 122708 (2010).

[35] A. K. Davis, D. Cao, D. T. Michel, M. Hohenberger, D. H. Edgell, R. Epstein, V. N. Goncharov, S. X. Hu, I. V. Igumenshchev, J. A. Marozas, A. V. Maximov, J. F. Myatt, P. B. Radha, S. P. Regan, T. C. Sangster, and D. H. Froula, Phys. Plasmas **23**, 056306 (2016).

[36] D. Turnbull, C. Goyon, G. E. Kemp, B. B. Pollock, D. Mariscal, L. Divol, J. S. Ross, S. Patankar, J. D. Moody, and P. Michel, Phys. Rev. Lett. **118**, 015001 (2017).

[37] A. M. Hansen, K. L. Nguyen, D. Turnbull, B. J. Albright, R. K. Follett, R. Huff, J. Katz, D. Mastrosimone, A. L. Milder, L. Yin, J. P. Palastro, and D. H. Froula, Phys. Rev. Lett. **126**, 075002 (2021).

[38] B. Xu and S. X. Hu, Phys. Rev. E **84**, 016408 (2011).

[39] J. Delettrez, R. Epstein, M. C. Richardson, P. A. Jaanimagi, and B. L. Henke, Phys. Rev. A **36**, 3926 (1987).

[40] P. B. Radha *et al.*, Phys. Plasmas **12**, 032702 (2005).

[41] V. Gopalaswamy *et al.*, Nature (London) **565**, 581+ (2019).